

# Role of electron-electron and electron-phonon interaction effect in the optical conductivity of VO<sub>2</sub>

K. Okazaki<sup>1</sup>, S. Sugai<sup>1</sup>, Y. Muraoka<sup>2</sup> and Z. Hiroi<sup>2</sup>

<sup>1</sup>*Department of Physics, Nagoya University, Nagoya 464-8602, Japan and*

<sup>2</sup>*Institute for Solid State Physics, University of Tokyo, Kashiwa 277-8581, Japan*

(Dated: February 6, 2008)

We have investigated the charge dynamics of VO<sub>2</sub> by optical reflectivity measurements. Optical conductivity clearly shows a metal-insulator transition. In the metallic phase, a broad Drude-like structure is observed. On the other hand, in the insulating phase, a broad peak structure around 1.3 eV is observed. It is found that this broad structure observed in the insulating phase shows a temperature dependence. We attribute this to the electron-phonon interaction as in the photoemission spectra.

PACS numbers: 71.30.+h, 71.20.Ps, 71.38.-k, 79.60.-i

## I. INTRODUCTION

The metal-insulator transition (MIT) is one of the most interesting phenomena in the strongly correlated electron systems.<sup>1</sup> VO<sub>2</sub> is well known for its first-order metal-insulator transition at 340 K,<sup>2</sup> which is accompanied by a structural transition. In the high temperature metallic phase it has a rutile structure, while in the low temperature insulating phase ( $M_1$  phase) the V atoms dimerize along the  $c$ -axis and the dimers twist, resulting in a monoclinic structure. The magnetic susceptibility changes from paramagnetic to nonmagnetic in going from the metallic to the insulating phase. Hence, this transition is analogous to a Peierls transition. In the early stage of the study for the MIT in VO<sub>2</sub>, Goodenough explained the MIT based on a simplified band model.<sup>3</sup> The V 3d  $t_{2g}$  level is split into the  $d_{||}$  and  $\pi^*$  sublevels due to the tetragonal crystal field. The  $\pi^*$  bands are hybridized with the O 2p bands and are pushed upward. The  $d_{||}$  band is rather weakly hybridized with the O 2p band and has the lowest energy among the V 3d bands. In the metallic phase, the  $\pi^*$  and  $d_{||}$  bands overlap and are partially filled. In the insulating phase, the  $\pi^*$  bands are shifted upward and the  $d_{||}$  band is split into two subbands. As a result, the  $\pi^*$  bands become empty and the lower  $d_{||}$  subband is completely filled.<sup>4</sup> However, this picture was criticized that only with the lattice distortion the optical gap of 0.6 eV<sup>5</sup> cannot be reproduced and the importance of electron correlation effect was pointed out based on the cluster calculations.<sup>6</sup> Zylbersztein and Mott claimed that while the insulating phase cannot be described correctly without taking into account of the electron correlation effect, for the metallic phase of VO<sub>2</sub>, the screening effect of the  $\pi^*$  bands on the  $d_{||}$  bands is important.<sup>7</sup>

On the basis of local-density approximation (LDA) band-structure calculation, Wentzcovitch *et al.*<sup>8</sup> concluded that the insulating phase of VO<sub>2</sub> is an ordinary band (Peierls) insulator. On the other hand, Cr-doped VO<sub>2</sub> or pure VO<sub>2</sub> under uniaxial pressure in the [110] direction of the rutile structure has another monoclinic in-

ulating phase called the  $M_2$  phase. In the  $M_2$  phase, half of the V atoms form pairs and the other half form zig-zag chains.<sup>9</sup> While the V atoms in the pairs are nonmagnetic, those in the zig-zag chains have local moments and are regarded as one-dimensional Heisenberg chains according to an NMR study.<sup>10</sup> Based on these observations for the  $M_2$  phase, Rice *et al.*<sup>11</sup> objected to Wentzcovitch *et al.* that the  $M_2$  phase is a Mott-Hubbard insulator and the  $M_1$  phase also must be classified as a Mott-Hubbard insulator. More recently, several theoretical studies have been reported for the MIT of VO<sub>2</sub>.<sup>12,13,14,15</sup> However, it still remains highly controversial whether the MIT of VO<sub>2</sub> is driven by the electron-phonon interaction (resulting in a Peierls insulator) or the electron-electron interaction (resulting in a Mott insulator).

To address this issue, both of the electron-electron and electron-phonon interaction effects should be further investigated. In a recent photoemission study, it is concluded that while the electron-electron interaction is necessary to produce the band gap in the insulating phase, the electron-phonon interaction is important to fully understand the electronic structure and charge transport in VO<sub>2</sub>.<sup>16</sup> To further understand how these effects are related to the charge transport, it is important to investigate the detailed charge dynamics of VO<sub>2</sub>. So far, several optical measurements have been reported for VO<sub>2</sub> using bulk samples<sup>5,17,18</sup> and thin film samples.<sup>18,19</sup> However, spectroscopic measurements are difficult for the metallic phase of VO<sub>2</sub> with the bulk crystals because the crystals break into pieces when it cross the MIT.<sup>20</sup> On the other hand, with the thin films, it is difficult to deduce the optical constants precisely from optical measurements because multiple reflections between the film and the substrate should be taken into account.

In this work, we report the optical conductivity of VO<sub>2</sub> at various temperatures deduced from the optical reflectivity measurements of TiO<sub>2</sub> substrates and VO<sub>2</sub> thin films grown on the TiO<sub>2</sub> substrate. It is observed that a broad Drude-like component in the metallic phase transfers to the higher energies around 1.3 eV in the insulating phase. We have also found that the structure around 1.3 eV in the insulating phase shows a temperature depen-

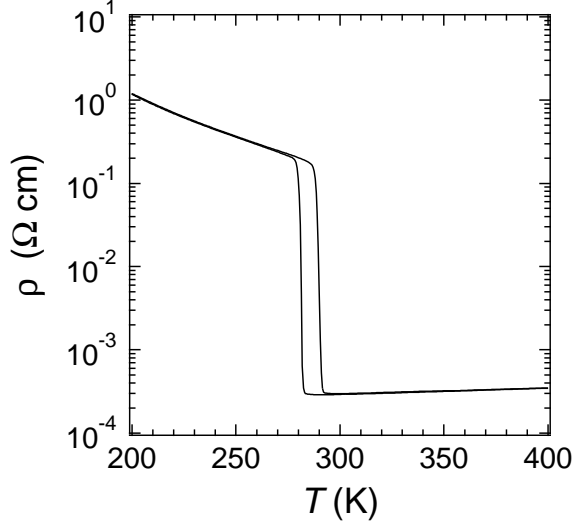


FIG. 1: Electrical resistivity  $\rho$  of  $\text{VO}_2/\text{TiO}_2$  (001) thin film. A jump of about three orders magnitude has been observed around 290 K.

dence similar to the photoemission spectra and considered that this is another evidence for the strong electron-phonon interaction.

## II. EXPERIMENTAL

$\text{VO}_2$  thin films were epitaxially grown on  $\text{TiO}_2(001)$  surfaces using the pulsed laser deposition technique as described in Ref. 21. The film thickness was  $\sim 100$  Å, estimated by four-cycle x-ray diffraction (XRD) measurements and the MIT was confirmed by electrical resistivity measurements (Fig. 1), showing a jump of about three orders of magnitude around 290 K ( $\equiv T_{MI}$ ). This reduced MIT temperature of the films is due to the compressive strain from the  $\text{TiO}_2$  substrate.<sup>21</sup>

Near-normal incidence optical reflectivity measurements were performed using a Fourier-type interferometer (0.006 - 1.2 eV) and a grating spectrometer (0.8 - 6.8 eV) from 5 K to 350 K. Because  $\text{VO}_2$  films have been epitaxially grown on the  $\text{TiO}_2$  (001) surface, polarization of the incident light is perpendicular to the  $c$ -axis of the Rutile structure ( $\mathbf{E} \perp c$ ). As a reference mirror, we used an evaporated Au film for the infrared regions and Ag film for the visible region. The experimental error of the reflectivity is less than 0.5 % for the far- and near-IR regions and less than 1.0 % for the mid-IR, visible and ultraviolet regions. A detailed procedure to deduce optical constants of  $\text{VO}_2$  from the reflectivity is described below.

The normal incidence complex reflectivity of the two layer system can be written as

$$\hat{r}(\omega) = \sqrt{R(\omega)} \cdot e^{i\Theta(\omega)}$$

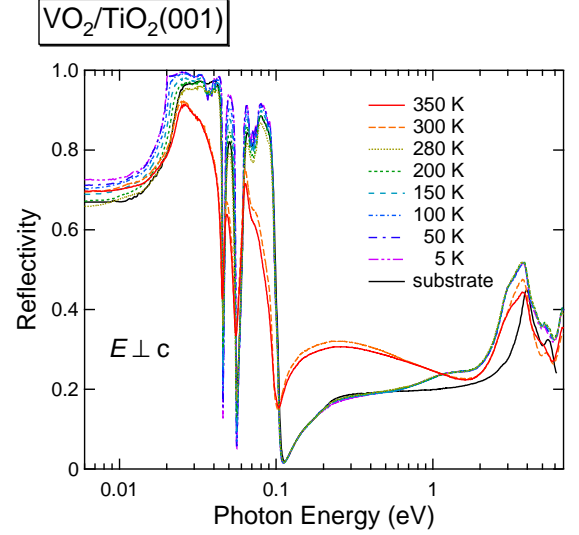


FIG. 2: Reflectivity spectra of  $\text{VO}_2/\text{TiO}_2$  (001) thin film at various temperatures. Below 0.1 eV, because the reflectivity of the substrate is large due to optical phonons, there is an interference effect between the reflection at the substrate and the film.

$$= \frac{\hat{r}_{0f} + \hat{r}_{fs}e^{2i\delta_f} + \hat{r}_{0f}\hat{r}_{fs}\hat{r}_{s0}e^{2i\delta_s} + \hat{r}_{s0}e^{2i(\delta_f+\delta_s)}}{1 + \hat{r}_{0f}\hat{r}_{fs}e^{2i\delta_f} + \hat{r}_{fs}\hat{r}_{s0}e^{2i\delta_s} + \hat{r}_{0f}\hat{r}_{s0}e^{2i(\delta_f+\delta_s)}}, \quad (1)$$

where

$$\begin{aligned} \hat{r}_{0f} &= [(n_f + ik_f) - 1]/[(n_f + ik_f) + 1], \\ \hat{r}_{fs} &= [(n_s + ik_s) - (n_f + ik_f)]/[(n_s + ik_s) + (n_f + ik_f)], \\ \hat{r}_{s0} &= [1 - (n_s + ik_s)]/[1 + (n_f + ik_f)], \\ \delta_f &= 2\pi i(n_f + ik_f)d_f/\lambda, \\ \text{and} \\ \delta_s &= 2\pi i(n_s + ik_s)d_s/\lambda. \end{aligned}$$

$n_f, k_f, d_f, n_s, k_s$ , and  $d_s$  are the refractive index, the extinction coefficient, and the film thickness of the film and the substrate, respectively and  $\lambda$  is the wave length of the incident light.

First, we have measured the reflectivity of the  $\text{TiO}_2$  substrates at various temperatures, and then obtained optical constants  $n_s$  and  $k_s$  using Kramers-Kronig (K-K) transformation. For the extrapolation to perform K-K transformation, we have assumed a constant value below 0.006 eV and a power-law behavior ( $\propto \omega^{-\alpha}$ ,  $0 < \alpha < 4$ ) above 6.8 eV. The value of  $\alpha$  was adjusted so that the obtained optical constants reproduced the reported values<sup>22</sup> at 300K. <sup>23</sup> Next, we have measured the reflectivity  $R(\omega)$  of the  $\text{VO}_2/\text{TiO}_2$  thin films as shown in Fig. 2 and deduced the phase shift  $\Theta(\omega)$  using K-K transformation. We have adopted a same assumption with the  $\text{TiO}_2$  substrate for the extrapolation. At last, we have obtained the optical constants  $n_f$  and  $k_f$  by numerically

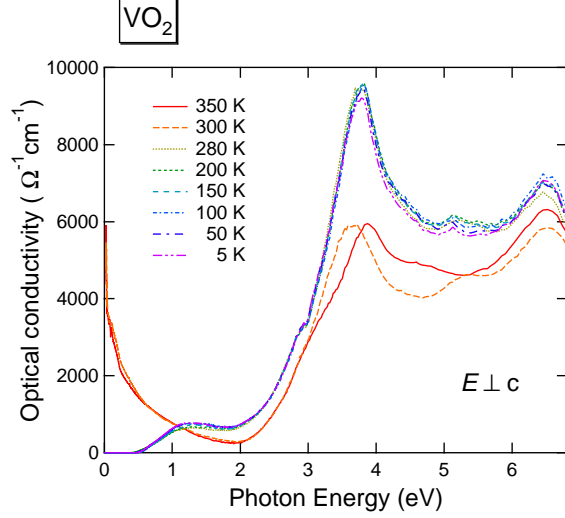


FIG. 3: Optical conductivity spectra of VO<sub>2</sub> at various temperatures deduced from the reflectivity spectra of VO<sub>2</sub>/TiO<sub>2</sub>(001) thin film.

solving the equations obtained from the real and imaginary part of Eq. (1) multiplied by the denominator of the right-hand side. When solving the equations, we have neglected the terms proportional to  $\sin(2\pi n_s d_s/\lambda)$  and  $\cos(2\pi n_s d_s/\lambda)$ . Because the substrate thickness  $d_s \sim 0.5$  mm is much larger than the wave length  $\lambda$  and is not uniform in the scale of  $\lambda$ , these terms can be replaced with their mean value zero.<sup>24</sup>

### III. RESULTS AND DISCUSSION

Figure 3 shows the optical conductivity spectra of VO<sub>2</sub> at various temperatures. The MIT is clearly observed as a spectral weight transfer of the broad Drude-like structure above  $T_{\text{MI}}$  to the Gaussian-like peak structure around 1.3 eV below  $T_{\text{MI}}$ . The structure around 1.3 eV can be assigned as a Mott-Hubbard excitation, while an intense peak around 3.8 eV, which is observed both above and below  $T_{\text{MI}}$ , can be assigned as a charge-transfer excitation.<sup>25</sup> In the metallic phase, the value of the optical conductivity in the low energy region is roughly in accordance with the DC conductivity ( $\sim 3500 \Omega^{-1}\text{cm}^{-1}$  at 300 K).

In Fig. 4, the number of the effective carriers ( $N_{\text{eff}}(\omega)$ ) defined as

$$N_{\text{eff}}(\omega) \equiv \frac{2m_0 V}{\pi e^2} \int_0^\omega \sigma(\omega') d\omega' \quad (2)$$

is shown, where  $m_0$  is the bare electron mass and  $V$  is the cell volume of the one formula unit. From  $N_{\text{eff}}$ , the spectral weight of the Drude-like component at 300 K can be estimated as 0.23 per formula unit. From this value, the plasma frequency  $\omega_p$  and the effective mass  $m^*$  can

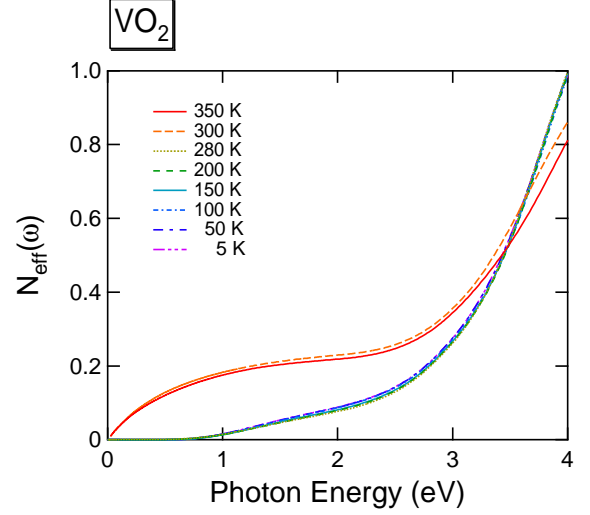


FIG. 4: Effective carrier number per formula unit  $N_{\text{eff}}$  of VO<sub>2</sub> obtained by integrating the optical conductivity.

be estimated using a so-called  $f$ -sum rule,

$$\int_0^{\omega_0} \sigma(\omega) d\omega = \frac{1}{8} \omega_p^2, \quad (3)$$

where  $\omega_p$  is defined as  $\omega_p^2 = 4\pi n e^2 / m^*$ ,  $\omega_0$  is taken as the energy for the upper limit of the contribution of the Drude-like component ( $= 2.0$  eV), and  $n$  is the charge density ( $= 1/V$  i.e., one electron per formula unit). Thus,  $\omega_p$  and  $m^*/m$  are estimated as 3.3 eV and 4.3, respectively. These values agree well with those estimated from the peak position of the energy-loss function  $\text{Im}(-1/\epsilon(\omega))$  by assuming its peak position corresponding to  $\omega_p/\sqrt{\epsilon_\infty}$ ,<sup>26</sup> where  $\epsilon_\infty$  is the optical dielectric constant and estimated as  $\sim 8$  from  $\text{Re}(\epsilon(\omega))$  at  $\omega = 2.0$  eV. The spectra of  $\text{Im}(-1/\epsilon(\omega))$  at 300 K has a peak at 1.15 eV and the  $\omega_p$  is estimated as 3.25 eV. From this consistency, we can say that the obtained mass enhancement factor  $m^*/m_0$  should be reasonable one. For another vanadium oxide  $d^1$  system  $\text{Sr}_{1-x}\text{Ca}_x\text{VO}_3$ , which is metallic at all temperatures,  $m^*/m_0$  has been estimated as  $\sim 3.1$  for  $\text{CaVO}_3$  and  $\sim 2.7$  for  $\text{SrVO}_3$  from optical measurements.<sup>27</sup> Hence,  $m^*/m_0$  of VO<sub>2</sub> is somewhat larger than that of  $\text{Sr}_{1-x}\text{Ca}_x\text{VO}_3$ . Hence, we can say that the quasiparticle renormalization or the electron correlation effect in VO<sub>2</sub> is stronger than  $\text{Sr}_{1-x}\text{Ca}_x\text{VO}_3$ . This is consistent with the quasiparticle renormalization factor  $Z$  estimated from photoemission spectroscopy. They have been estimated as  $\sim 0.3$  for VO<sub>2</sub> (Ref.16) and  $\sim 0.5$  for  $\text{Sr}_{1-x}\text{Ca}_x\text{VO}_3$  (Ref.29), respectively.

Using the value of  $\omega_p$  estimated above, we have compared the optical conductivity at 300 K with the simple Drude model with various  $\gamma$  (scattering rate) in Fig. 5. In the simple Drude model, the optical conductivity is given by  $\sigma(\omega) = \omega_p^2 \gamma / 4\pi(\omega^2 + \gamma^2)$ . With a larger value of

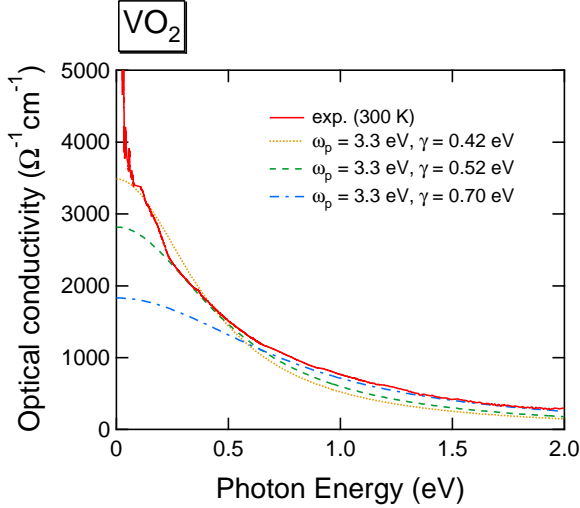


FIG. 5: Comparison of the optical conductivity of VO<sub>2</sub> in the metallic phase with the simple Drude model.

$\gamma$ , the simple Drude model seem to fit in the higher energy region. However, it cannot reproduce the whole line shape of the optical conductivity with the only one value. This should correspond to the energy dependence of the  $\gamma$ . Then, we introduce the energy dependence in  $\gamma$  and  $m^*/m_0$  using the extended Drude model. Figure 6 shows  $\gamma(\omega)$  and  $m^*(\omega)/m_0$  at 300 K above 0.1 eV. As expected from the comparison with the simple Drude model,  $\gamma(\omega)$  increases with the photon energy and is almost proportional to  $\omega$ , while the energy dependence of  $m^*(\omega)/m_0$  is not so large. A similar behavior has been observed in other transition-metal oxides.<sup>27,30</sup> However, it seems to be a still open question why  $\gamma(\omega)$  is proportional to  $\omega$  rather than  $\omega^2$  as expected from the standard Fermi liquid theory.

Although the behavior of  $\gamma(\omega) \propto \omega$  is commonly observed in other transition-metal oxides, the value of  $\gamma(\omega)$  of VO<sub>2</sub> is somewhat larger compared to Sr<sub>1-x</sub>Cr<sub>x</sub>VO<sub>3</sub>. For the case of VO<sub>2</sub>, this feature may be related to the temperature dependence of the electronic resistivity. Allen *et al.*<sup>31</sup> have reported that the resistivity of the single crystal VO<sub>2</sub> shows a linear temperature dependence and does not saturate at least up to 840 K. They have estimated the mean free path  $\sim 3$  Å at 800 K and claimed that VO<sub>2</sub> might not be a conventional Fermi liquid. When the mean free path is such small, description for the electronic transport by the Boltzmann equation may be not valid. However, the unexpected small mean free path is due to the large scattering rate and hence, these features in the electronic resistivity and the optical conductivity may be related to the characteristic scattering mechanism in VO<sub>2</sub>.

Next, we would like to discuss the optical conductivity spectra in the insulating phase. Figure 7 shows the optical conductivity spectra of VO<sub>2</sub> in the region of the Mott-

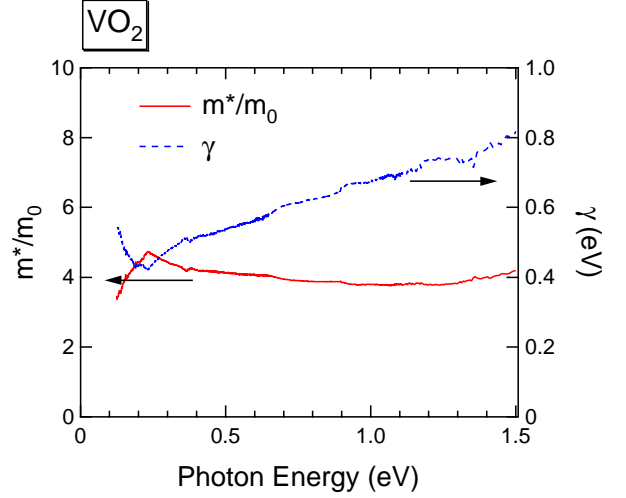


FIG. 6: Energy-dependent mass enhancement factor  $m^*(\omega)/m_0$  and the scattering rate  $\gamma(\omega)$  deduced from the extended Drude model.

Hubbard excitation. The contribution from the higher energy peak is subtracted by assuming as shown in the inset. We would like to note that the peak position of this excitation is far less than twice of the peak position of V 3d peak of the photoemission spectra ( $\sim 1.0$  eV). For example, the dynamical mean field theory (DMFT) predicts that the spectral function of the half-filled Hubbard model has peaks at  $\omega = -U/2$  and  $U/2$  corresponding the lower- and upper-Hubbard band, respectively and that the optical conductivity has a peak at  $\omega = U$  in the insulating region. In fact, Sr<sub>1-x</sub>Ca<sub>x</sub>VO<sub>3</sub> and V<sub>2</sub>O<sub>3</sub> have been interpreted within this scheme.<sup>27,28</sup> For the case of VO<sub>2</sub>, the different  $d$ -electron bands,  $d_{||}$  and  $\pi^*$  bands<sup>3</sup> could be related to this transition. Because the polarization of the incident light is  $\mathbf{E} \perp c$ , the occupied  $d_{||}$  orbitals cannot transfer to the nearest neighbor V atoms along  $c$ -axis (See Fig. 8). Hence, this structure is assigned to the  $d$ - $d$  transfer to the second nearest neighbor V atoms. Furthermore,  $d_{||}$  orbitals between the second-nearest-neighbor V atoms are orthogonal, this structure should be the  $d_{||}$ - $\pi^*$  transition between the second-nearest-neighbor V atoms.

The spectra in Fig. 7 have the similar line shapes and show a similar temperature dependence to the photoemission spectra. Because the optical conductivity spectra in Fig. 3 show almost no temperature dependence around the region from 2.5 eV to 3.0 eV in the insulating phase, the same Gaussian function was used to subtract the contribution from the higher energy peak for all the spectra in Fig. 7. Hence, this subtraction procedure does not affect the temperature dependence below 2.5 eV. In the recent photoemission study,<sup>16</sup> the line shape of the V 3d band and its temperature dependence has been reproduced by the independent boson model and attributed to the strong electron-phonon coupling. Using the independent boson model, the optical conductivity at finite

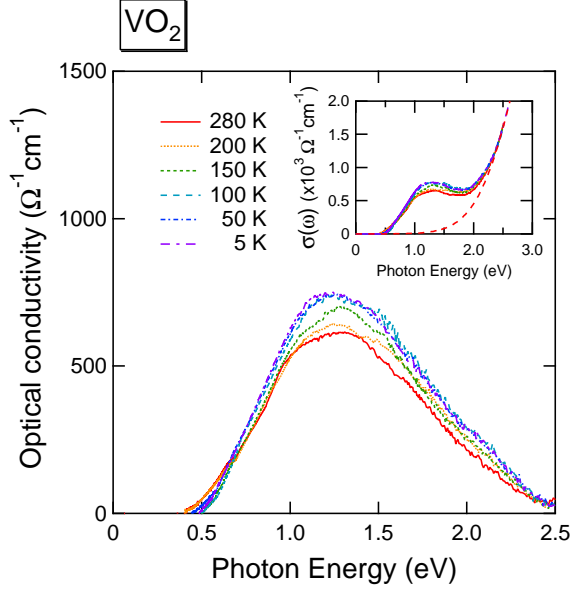


FIG. 7: Temperature dependence of the optical conductivity of VO<sub>2</sub> in the insulating phase in the region of Mott-Hubbard excitation after subtraction of the the contribution from the higher-energy peak.

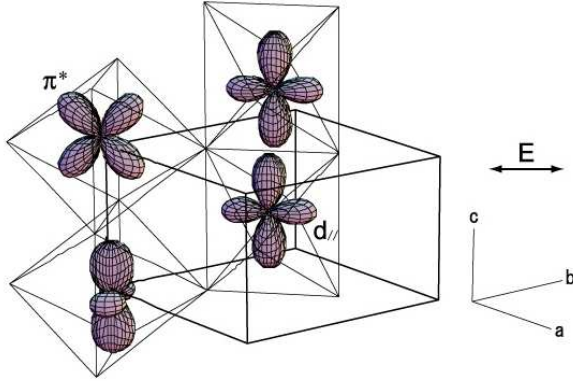


FIG. 8: Configuration between the  $d_{||}$  and  $\pi^*$  orbitals. The occupied  $d_{||}$  orbitals can transfer to the unoccupied  $\pi^*$  orbitals of the second-nearest-neighbor V atom with the  $\mathbf{E} \perp c$  polarization, while it cannot transfer to the  $d_{||}$  orbitals of the nearest and the second-nearest-neighbor V atoms. Thick lines indicate the unit cell of the rutile structure and thin lines indicate oxygen octahedra. (Note that the unit cell volume in the insulating phase is twice of the rutile structure in the metallic phase.)

temperature can be written by a similar expression to the

spectral function,<sup>32</sup>

$$\sigma(\omega) \propto \frac{\pi}{\omega} e^{-g_{if}(2N+1)} \sum_l \frac{g_{if}^l}{l!} \sum_{m=0}^l {}_lC_m N^m (N+1)^{l-m} \times \delta(\omega - \varepsilon_i + \varepsilon_f + \Delta_i - \Delta_f - (l-2m)\omega_0).$$

This describes a transition from the initial state  $i$  to the final state  $f$ .  $N$  is the phonon occupation number,  $g_{if}$  is the effective electron-phonon coupling constant, which is dependent on the electron-phonon coupling of both the initial and final states,  $\omega_0$  is the phonon energy,  $\varepsilon_i$  and  $\varepsilon_f$  are the energies of the initial and final states, respectively, and  $\Delta_i$  and  $\Delta_f$  are the electron self-energies of the initial and final states, respectively. From this expression, similar temperature dependence to the photoemission spectra is expected for the optical conductivity. Hence, we conclude that the temperature dependence of the optical conductivity is another evidence for the strong electron-phonon interaction.

#### IV. CONCLUSION

We have studied the charge dynamics of VO<sub>2</sub> by the optical reflectivity measurements. The optical conductivity clearly shows a metal-insulator transition. In the metallic phase, the spectral weight of the Drude-like component and the mass enhancement factor  $m^*/m_0$  have been estimated as  $\sim 0.23$  and 4.3, respectively. This  $m^*/m_0$  is somewhat larger than another  $d^1$  vanadium oxide Sr<sub>1-x</sub>Ca<sub>x</sub>VO<sub>3</sub>. From this, we have concluded that the electron correlation effect in VO<sub>2</sub> is stronger than Sr<sub>1-x</sub>Ca<sub>x</sub>VO<sub>3</sub>. From the extended Drude model,  $\gamma(\omega)$  is rather large and almost proportional to  $\omega$ . This would be related to the characteristic scattering mechanism in the metallic phase of VO<sub>2</sub>. In the insulating phase, the broad Gaussian-like structure has been observed around 1.3 eV. This would be a  $d_{||}$ - $\pi^*$  transition between the second-nearest-neighbor V atoms. This structure show a similar temperature dependence to the photoemission spectra. We have concluded that this is another evidence for the strong electron-phonon coupling.

#### Acknowledgements

The authors would like to thank J. Matsuno and A. Fujimori for enlightening discussions. This work was partially supported by the 21st Century COE program of Nagoya University and Grant-in-Aid for Scientific Research from the Ministry of Education, Culture, Sports, Science and Technology, Japan.

<sup>1</sup> M. Imada, A. Fujimori, and Y. Tokura, Rev. Mod. Phys. **70**, 1039 (1998).

<sup>2</sup> J. Morin, Phys. Rev. Lett. **3** (1959).

- <sup>3</sup> J. B. Goodenough, J. Solid State Chem. **3**, 490 (1971).
- <sup>4</sup> See Fig. 3 and Fig. 4 in Ref. 3.
- <sup>5</sup> L. Ladd and W. Paul, Solid State Commun. **7** 425 (1969).
- <sup>6</sup> C. Sommers, R. de Groot, D. Kaplan, and A. Zylbersztejn, J. de Phys. Lett. **36**, L-157 (1975); C. Sommers and S. Doniach, Solid State Commun. **28**, 133 (1978).
- <sup>7</sup> A. Zylbersztejn and N. F. Mott, Phys. Rev. B, **11**, 4384 (1975).
- <sup>8</sup> R. M. Wentzcovitch, W. W. Schulz, and P. B. Allen, Phys. Rev. Lett. **72**, 3389 (1994).
- <sup>9</sup> M. Marezio, D. B. McWhan, J. P. Remeika, and P. D. Dernier, Phys. Rev. B **5**, 2541 (1971).
- <sup>10</sup> J. P. Pouget, H. Launois, T. M. Rice, P. Dernier, A. Gossard, G. Villeneuve, and P. Hagenmuller, Phys. Rev. B **10**, 1801 (1974).
- <sup>11</sup> T. M. Rice, H. Launois, and J. P. Pouget, Phys. Rev. Lett. **73**, (1994) 3042.
- <sup>12</sup> A. Tanaka, J. Phys. Soc. Jpn. **72**, 2433 (2003).
- <sup>13</sup> S. Biermann, A. Poteryaev, A. I. Lichtenstein, and A. Georges, Phys. Rev. Lett. **94**, 026404 (2005).
- <sup>14</sup> A. Liebsch, H. Ishida, and G. Bihlmayer, Phys. Rev. B **71**, 085109 (2005).
- <sup>15</sup> M. S. Laad, L. Craco, and E. Muller-Hartmann, Europhys. Lett. **69** 984 (2005).
- <sup>16</sup> K. Okazaki, H. Wadati, A. Fujimori, M. Onoda, Y. Muraoka, and Z. Hiroi, Phys. Rev. B **69**, 165104 (2004).
- <sup>17</sup> A. S. Barker, Jr., H. W. Verleur, and H. J. Guggenheim, Phys. Rev. Lett. **17**, 1286 (1966).
- <sup>18</sup> H. W. Verleur, A. S. Barker, Jr., and C. N. Berglund, Phys. Rev. **172**, 788 (1968).
- <sup>19</sup> H. S. Choi, J. S. Ahn, J. H. Jung, and T. W. Noh, and D. H. Kim, **54**, 4621 (1996).
- <sup>20</sup> K. Okazaki, A. Fujimori, and M. Onoda, J. Phys. Soc. Jpn. **71**, 822 (2002).
- <sup>21</sup> Y. Muraoka and Z. Hiroi, Appl. Phys. Lett., **80**, 583 (2002).
- <sup>22</sup> M. W. Ribarsky, in *Handbook of Optical Constants of Solids*, edited by E.D. Palik (Academic Press, Orlando, 1985).
- <sup>23</sup> F. Woooten, *Optical Properties of Solids* (Academic Press, New York and London, 1972).
- <sup>24</sup> P. -O. Nilsson, Appl. Opt. **7**, 435 (1968).
- <sup>25</sup> T. Arima, Y. Tokura, and J. B. Torrance, Phys. Rev. B **48**, 17006 (1993).
- <sup>26</sup> Strictly, even in the simple Drude model, only when  $\gamma$  is small enough, the peak position of the energy-loss function is located at  $\omega_p/\sqrt{(\epsilon_\infty)}$ .
- <sup>27</sup> H. Makino, I. H. Inoue, M. J. Rozenberg, I. Hase, Y. Aiura, and S. Onari, Phys. Rev. B **58**, 4384 (1998).
- <sup>28</sup> M. J. Rozenberg, G. Kotliar, H. Kajueter, G. A. Thomas, D. H. Rapkine, J. M. Honig, and P. Metcalf, Phys. Rev. Lett. **75**, 105 (1995).
- <sup>29</sup> A. Sekiyama, H. Fujiwara, S. Imada, S. Suga, H. Eisaki, S. I. Uchida, K. Takegahara, H. Harima, Y. Saitoh, I. A. Nekrasov, G. Keller, D. E. Kondakov, A.V. Kozhevnikov, Th. Pruschke, K. Held, D. Vollhardt, and V. I. Anisimov, Phys. Rev. Lett. **93**, 156402 (2004).
- <sup>30</sup> T. Katsufuji, Y. Okimoto, T. Arima, Y. Tokura, and J. B. Torrance, Phys. Rev. B **51**, 4830 (1995).
- <sup>31</sup> P. B. Allen, R. M. Wentzcovitch, W. W. Schulz, and P. C. Canfield, Phys. Rev. B **48**, 4359 (1993).
- <sup>32</sup> G. D. Mahan, *Many-Particle Physics*, (Plenum, New York, 1981) Sec. 4.3.